Temperature dependent forward current-voltage characteristics of Ni/Au Schottky contacts on AlGaN/GaN heterostructures described by a two diodes model

Giuseppe Greco, Filippo Giannazzo, and Fabrizio Roccaforte
Consiglio Nazionale delle Ricerche - Istituto per la Microelettronica e Microsistemi (CNR-IMM), Strada VIII n. 5- Zona industriale, 95121 Catania, Italy

(Received 7 October 2016; accepted 11 January 2017; published online 24 January 2017)

This paper reports on the temperature dependence of Ni/Au Schottky contacts on AlGaN/GaN heterostructures. The electrical properties of the Schottky barrier were monitored by means of forward current-voltage (I–V) measurements, while capacitance-voltage measurements were used to determine the properties of the two dimensional electron gas. The forward I–V characteristics of Schottky diodes revealed a strong deviation from the ideal behavior, which could not be explained by a standard thermionic emission model. Thus, the Ni/AlGaN/GaN system has been described by a "two diode model," considering the presence of a second barrier height at the AlGaN/GaN heterojunction. Following this approach, the anomalous I–V curves could be explained and the value of the flat-band barrier height (at zero-electric field) could be correctly determined, thus resulting in good agreement with literature data based on photoemission measurements. *Published by AIP Publishing*. [http://dx.doi.org/10.1063/1.4974868]

I. INTRODUCTION

Wide band gap AlGaN/GaN heterostructures are considered to be excellent systems to fulfill the demands of future RF power devices, in terms of power density, operation speed, and energy efficiency.[1] In fact, the high critical electric field of GaN and related $Al_xGa_{1-x}N$ alloys, combined with the presence of a two dimensional electron gas (2DEG) at AlGaN/GaN interfaces,[2] permits the fabrication of high electron mobility transistors (HEMTs) with a low specific on-resistance (few $m\Omega\ cm^2$) at high breakdown voltages (600–1200 V)[3] or high frequency operation ($f_T > 200$ GHz) for low voltages applications.[4] In addition, the large band gap of $Al_xGa_{1-x}N$ alloys, tunable with the Al-concentration, makes them also suitable for the fabrication of efficient solar-blind UV-detectors.[5]

In this context, the knowledge of the transport properties at metal/AlGaN interfaces is of fundamental interest, as Schottky contacts are the main building block for the functionality of these devices.

Metal/semiconductor Schottky barriers have been widely investigated on n-type GaN in the last two decades.[6–11] In general, the classical thermionic emission (TE) or thermionic field emission (TFE) models have been used to describe the transport mechanisms at metal/GaN interfaces from the temperature dependence of Schottky diodes characteristics.[12–17] Moreover, the role of surface processing,[18,19] post-annealing conditions,[20] and material defects[14,21–23] has been widely discussed.

On the other hand, metal/semiconductor contacts on AlGaN/GaN heterostructures have attracted more interest only during the most recent years. Several works on HEMT structures were focused on Schottky barriers formed with high work-function metals (Pt, Ni,…) to obtain a high barrier height and reduce the leakage current.[9,24,25] In this case, the temperature dependence of the I-V characteristics of Schottky contacts on AlGaN/GaN heterostructures was explained either using TE[26] or tunneling-based mechanisms,[13] pointing out that carrier tunneling mechanisms can be enhanced in the presence of a high density of material defects (e.g., dislocations), leading to significant deviations from the ideal behavior.[27–29]

In spite of such a large number of works, the transport mechanism at Schottky contacts on AlGaN/GaN heterostructures still remains a debated topic, since the presence of the heterojunction with the 2DEG can influence the overall barrier properties and must be properly considered.

In this context, some authors recently proposed more accurate descriptions of metal/semiconductor Schottky barriers on AlGaN/GaN heterostructures, taking into account the effects of polarization charges and the presence of the 2DEG.[30,31] Chen *et al.*[32] proposed a "two diode model" for the AlGaAs/GaAs systems, which was recently used by Lv *et al.*[33] to describe the forward current-voltage (I-V) characteristics of AlGaN/GaN Schottky diodes measured at room temperature. However, in these works, the temperature dependence of the barrier parameters has not been considered, as well as any influence of the metal/semiconductor contact on the 2DEG properties.

In this paper, the temperature dependence of the forward I–V characteristics of Ni/Au Schottky contacts on AlGaN/GaN heterostructures has been described adapting "the two diode model" to consider the effect of the 2DEG at the heterojunction. This model allowed us to explain the non-ideal behavior of the I–V curves. Moreover, the study of the temperature dependent I–V characteristics, combined with experimental C-V measurements, provided a correct determination of the Ni/AlGaN barrier height, introducing the flat-band barrier height. The results obtained with this

method based on electrical measurements were corroborated by the comparison with literature photoemission data.

II. EXPERIMENTAL

In this work, AlGaN/GaN heterostructures grown on silicon substrates were used. The AlGaN barrier layer had a thickness $d = 20\,nm$ and an Al-concentration of 24%. Schottky diodes were fabricated on these samples in order to study the properties of the Ni/AlGaN barrier. In particular, first Ohmic contacts have been formed using a Ti/Al/Ni/Au (15/200/50/50 nm) stack annealed at 850 °C in Ar.[34] Then, circular Schottky contacts have been fabricated by deposition of a Ni/Au (50/50 nm) bi-layer. Such structures consist of an inner circular Schottky contact of radius of 150 μm and an Ohmic contact formed by a circular ring, which surrounds the Schottky electrode. The metal has been subjected to a Rapid Thermal Annealing (RTA) at 400 °C in Ar for 60 s in a Jipelec JetFirst furnace, in order to improve the metal/semiconductor interface quality and to reduce the series resistance.[35]

To determine the mechanism of current transport and get insights into the metal/semiconductor barrier properties, forward current-voltage (I–V) measurements have been carried out at different temperatures, in the range of 25–150 °C. Moreover, capacitance-voltage (C-V) measurements have been acquired, in order to get information on the heterostructure properties, extracting the experimental sheet charge density of the 2DEG at the AlGaN/GaN interface. A Karl Suss Microtec probe station equipped with HP 4156B and Agilent B5105 parameter analyzers has been used for electrical measurements.

III. RESULTS AND DISCUSSION

The I–V characteristics of Schottky contacts on n-type GaN are often described with the TE model[36]

$$I = SA^{*}T^{2}e^{-\frac{\Phi_B}{kT}}\left(e^{\frac{qV}{nkT}} - 1\right), \quad (1)$$

where S is the contact area, A^{*} is the Richardson constant, k is the Boltzmann constant, and Φ_B and n are the Schottky barrier height and the ideality factor, respectively.

In Fig. 1, the forward I–V characteristics of the Ni/Au Schottky diodes fabricated on AlGaN/GaN heterostructures are shown at different temperatures. Evidently, the electrical characteristics exhibit a strongly non-ideal behavior, as can be deduced by the presence of the two regions (Reg. I and Reg. II) with different slopes in the semi-log plot of the I–V curves between 0.5 and 2 V.

A linear fit of the experimental forward I–V curves in the Reg. I has been carried out at each temperature, applying the TE theory (Eq. (1)), in order to have a preliminary estimation of the values of the barrier height $\Phi_{B1}{}^{TE}$. As an example, at room temperature, a value of $\Phi_{B1}{}^{TE} = 0.77\,eV$ was determined, which is lower compared to the value of 0.96 eV obtained by Saadaoui *et al.*[26] in similar samples. For our calculation, the theoretical value of the Richardson constant for AlGaN ($A^{*} = 32\,A/(cm^2\,K^2)$[29]) has been used. However, it is known that the Richardson constant is very sensitive to the metal/semiconductor interface homogeneity,[37,38] and large scattering in its values has been reported for GaN.[23] As a matter of fact, high values of the ideality factor ($n > 2$) have been extracted in the entire temperature range in our system. Arslan *et al.*[28] correlated the high ideality factor with the high density of dislocations in the material. On the other hand, Yan *et al.*[29] justified the strong deviation from the ideality invoking a combination of different current transport mechanisms.

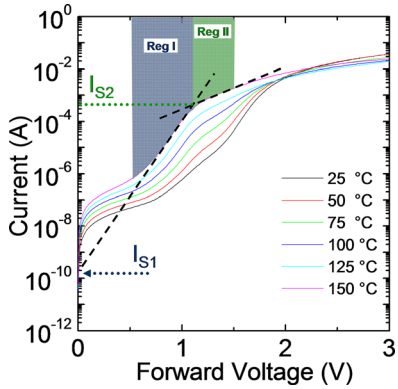

FIG. 1. Temperature dependence of the forward I-V characteristics of Ni/Au Schottky contacts on AlGaN/GaN heterostructures. The presence of two regions with different slopes is highlighted. The dashed lines represent the linear fits carried out in the two regions to extract the saturation currents of the two diodes (I_{S1} and I_{S2}).

As can be seen in Fig. 2, both parameters exhibit a strong dependence on the temperature, i.e., Φ_B increases with increasing temperatures, while n decreases with the temperature. This behavior is an indication of a strong inhomogeneity of the metal/semiconductor barrier on the AlGaN/GaN heterostructure. Hence, the value of the barrier height $\Phi_{B1}{}^{TE}$ estimated by the linear fit in Reg. I can be inaccurate, as the TE theory does not fully consider the complexity of the AlGaN/GaN system.

On the other hand, at higher voltage bias, a second region (Reg. II) can be identified. In this region, the I–V curves change their original slope. The electrical behaviour observed in Reg. II cannot be explained simply considering the TE model. Hence, to give a more exhaustive description

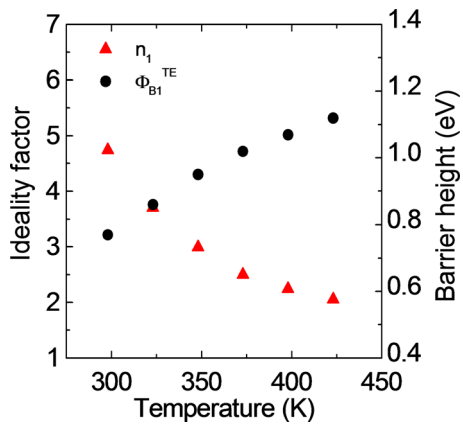

FIG. 2. Temperature dependence of the ideality factor n_1 and of the barrier height $\Phi_{B1}{}^{TE}$ determined by the standard thermionic-emission (TE) model, fitting the I–V curves reported in Fig. 1 in the Reg. I.

of our system, explaining also the presence of this second region, we have adapted to the AlGaN/GaN heterostructure the "two diode model" originally proposed by Chen *et al.*[32] to describe the AlGaAs/GaAs system.

Hence, to give a more exhaustive description of our system, we have adapted to the AlGaN/GaN heterostructure the "two diode model" originally proposed by Chen *et al.*[32] to describe the AlGaAs/GaAs system.

Accordingly, the metal/AlGaN/GaN system can be thought as the series of two diodes in a "back-to-back" configuration. Then, the equivalent circuit will be formed by a first forward biased diode (D_1), which corresponds to the metal/AlGaN interface, and a second reverse biased diode (D_2), which is related to the AlGaN/GaN interface, as illustrated in Fig. 3(a). The schematic representations of the conduction band diagrams of the "two diode model" at zero-bias ($V = 0\,V$), at the flat-band voltage condition ($V = V_{FB}$), and above the flat-band voltage ($V > V_{FB}$) are depicted in Figs. 3(b), 3(c), and 3(d), respectively. In the three diagrams, Φ_{B1} is the barrier height formed at the metal/AlGaN interface, analogous to the barrier typically used for the standard description of metal/semiconductor interfaces, whereas Φ_{B2} is the energy difference between the GaN conduction band edge and the Fermi level E_F of the AlGaN/GaN 2DEG. Since the position of the Fermi level with respect to the minimum of the AlGaN/GaN potential well depends on the applied bias, Φ_{B2} results to be slightly dependent on V. Hence, $\Phi_{B2}(0)$ in Fig. 2(b) represents the value of Φ_{B2} at zero-bias, whereas $\Phi_{B2}(V_{FB})$ in Fig. 3(c) is its value at the flat-band voltage condition. At zero-bias, the Fermi level of the metal contact and that of the AlGaN/GaN 2DEG are aligned, whereas at the flat-band condition the electric field becomes zero.

The behavior of the I–V characteristics measured on the Ni/AlGaN/GaN Schottky diode can be described according to the above discussed band diagrams as follows. The bias V applied to the system can be expressed as the sum of the voltage drop on diode D_1 and that on diode D_2 ($V = V_1 + V_2$). However, for low values of the applied voltage ($V < V_{FB}$), all the bias will drop on the first barrier Φ_{B1} ($V = V_1$). Then, by increasing the voltage above V_{FB}, a part of the bias (V_2) will drop on the second reversed biased diode D_2 with barrier height Φ_{B2}. Finally, the series resistance will become dominant by a further increase in the applied voltage, as can be seen in Fig. 1 from the bending of the I–V curves above 2 V. The two current transport regions can be identified through the occurrence of the two slopes in the I–V curves.

For the first diode D_1, which is under forward bias, the current in the Reg. I (i.e., for $V_1 \gg kT/q$) can be expressed as

$$I_{D1} = SA^*T^2 e^{-\frac{\Phi_{B1}(0)}{kT}} e^{\frac{qV_1}{n_1 kT}} = I_{S1} e^{\frac{qV_1}{n_1 kT}}, \tag{2}$$

where n_1 is the ideality factor of diode D_1 and $\Phi_{B1}(0)$ is the zero-bias barrier height. In Eq. (2), I_{S1} is the saturation current of diode D_1, which can be determined by a linear fit of the I–V curves in the Reg. I, as indicated in Fig. 1.

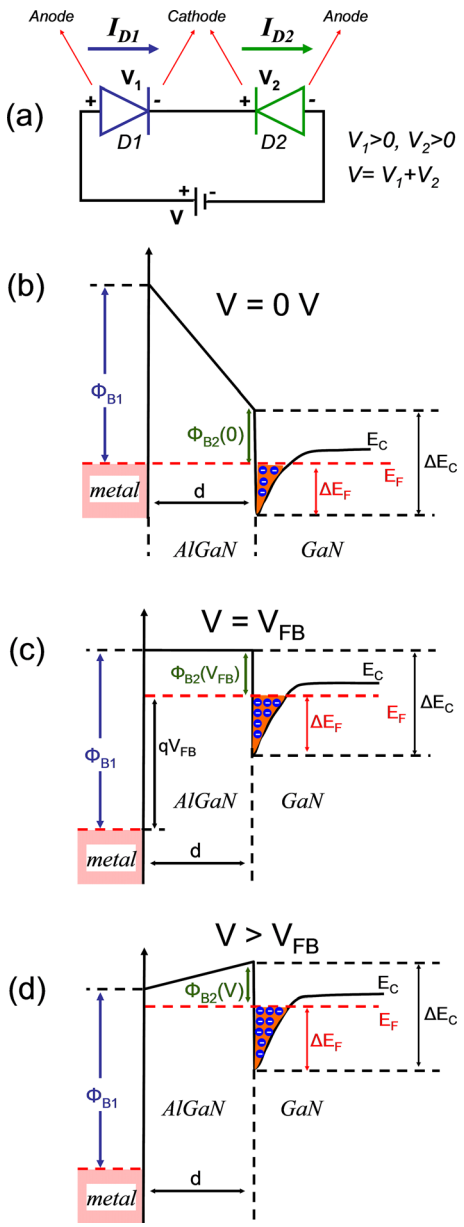

FIG. 3. Schematic representation of the "two diode model" equivalent circuit (a) and of the conduction band diagram of the AlGaN/GaN heterostructure at zero-bias $V = 0\,V$ (b), at the flat-band voltage $V = V_{FB}$ (c), and above the flat-band condition $V > V_{FB}$ (d).

As can be observed in the schematic band diagram reported in Fig. 3, the current of diode D_2 depends on how the second barrier height varies with the applied bias. In particular, considering the schematic of the circuit reported in Fig. 3(a), it is possible to write the current of diode D_2 as

$$I_{D2} = SA^*T^2 e^{-\frac{\Phi_{B2}(V_2)}{kT}} \left(e^{\frac{qV_2}{n_2 kT}} - 1 \right), \tag{3}$$

where $\Phi_{B2}(V_2)$ is the bias-dependent barrier height seen by the carriers at the AlGaN/GaN interface, V_2 is the voltage drop on the diode D_2, and n_2 is the ideality factor of this diode.

Note that, a minus sign of the current and of the voltage drop V_2 should be present in Eq. (3) to take into account the polarity of the equivalent circuit. However, as pointed out by

Chen *et al.*,[32] the sign could be neglected in the entire formalism, assuming that the current flows from the terminal with a more positive bias to the terminal with lower bias (see Fig. 3(a)).

Then, for the reversely biased diode D_2, when the voltage drop V_2 is larger than kT/q, the current can be approximated as

$$I_{D2} \approx SA^*T^2 e^{\frac{\Phi_{B2}(V_2)}{kT}}. \quad (4)$$

Under these conditions, the bias-dependent barrier height $\Phi_{B2}(V_2)$ appearing in Eq. (4) can be expanded by a first order Taylor series as

$$\Phi_{B2}(V_2) = \Phi_{B2}(0) - \left(\frac{\partial \Phi_{B2}}{\partial V_2}\right) V_2 = \Phi_{B2}(0) - \left(\frac{1}{n_2}\right) V_2, \quad (5)$$

where $\Phi_{B2}(0)$ is the zero-bias barrier height of the diode D_2 (which depends only on the heterostructures properties) and $\frac{\partial \Phi_{B2}}{\partial V_2}$ gives the voltage dependence of the barrier Φ_{B2}. The variation of the barrier height with the voltage drop can be considered as the inverse of the ideality factor n_2 of the second diode D_2.

Therefore, by combining Eq. (4) with Eq. (5), the current of the diode D_2 can be rewritten as

$$I_{D2} = SA^*T^2 e^{-\frac{\Phi_{B2}(0)}{kT}} e^{\frac{qV_2}{n_2 kT}} = I_{S2} e^{\frac{qV_2}{n_2 kT}}. \quad (6)$$

It is worth noting that, although Eq. (6) is valid only when diode D_2 is under reverse bias, it formally appears as the equation of a Schottky diode under forward bias, where I_{S2} can be determined by fitting the Reg. II of the experimental I–V curves.

Clearly, as the external bias applied to the system drops on the two diodes, the correct extrapolation of I_{S2} is obtained from the interception of the linear fit of the diode D_2 with that of the diode D_1, as graphically shown in Fig. 1 for the curve acquired at 150 °C. It is worth noting that the abscissa of the intersection point between these two fits represents the flat-band voltage V_{FB}, which is only slightly dependent on the temperature ($V_{FB} = 1.12$ eV at 25 °C and $V_{FB} = 1.14$ eV at 150 °C).

From the expressions of the saturation current I_{S1} and I_{S2} of Eqs. (2) and (6), an expression for $\Phi_{B1}(0)$ can be derived

$$\Phi_{B1}(0) = \frac{kT}{q} \ln\left(\frac{I_{S2}}{I_{S1}}\right) + \Phi_{B2}(0). \quad (7)$$

It is worth noting that the calculation of $\Phi_{B1}(0)$ from Eq. (7) does not require the knowledge of the Richardson constant, as reported in the previous works.[32,33] However, to evaluate $\Phi_{B1}(0)$ from Eq. (7), it is necessary to know the barrier height at the second diode $\Phi_{B2}(0)$, which in turn is an important physical parameter that depends on the heterostructure properties, i.e.,

$$\Phi_{B2}(0) = \Delta E_C - \Delta E_F, \quad (8)$$

where ΔE_C is the band gap discontinuity between GaN and AlGaN at the interface, and $\Delta E_F = E_F(0) - E_{Cmin}$ is the position of the Fermi level at zero bias with respect to the GaN conduction band at the interface (see Fig. 2(c)).

In the model proposed by Chen *et al.*[32] and later by Lv *et al.*,[33] the barrier height $\Phi_{B2}(0)$ was calculated by an iterative procedure involving the self-consistent solution of Schrodinger's and Poisson's equations. On the other hand, in the present work, we propose a more straightforward approach based on the experimental determination of the 2DEG properties (by C-V measurements), which takes into account the presence of the fabricated Schottky contact on the top of the barrier AlGaN layer.

In particular, for our Al-concentration of 24% a band discontinuity $\Delta E_C = 0.32$ eV has been considered, according to the relation[2,39]

$$\Delta E_C = 0.7\left[E_{gap}(x_{Al}) - E_{gap}(0)\right]. \quad (9)$$

On the other hand, the dependence of ΔE_F on the applied bias can be experimentally determined by C-V measurements carried out on the same lateral Schottky diodes used for I–V measurements. In fact, by integrating the C-V curves it is possible to determine the experimental sheet carrier concentration n_S of the 2DEG as a function of the applied voltage. The experimental C-V curve measured on the diode in the depletion regime ($V < 0$) and the corresponding sheet carrier density n_S are reported in Fig. 4. The dependence of ΔE_F on the applied bias can be determined inserting the experimental value of n_S in the relation[2]

$$\Delta E_F = \frac{\pi \hbar^2}{q m^*} n_S + \frac{1}{q}\left(\frac{9\pi \hbar q^2}{8\varepsilon_0 \varepsilon_{AlGaN}\sqrt{8m^*}}\right)^{2/3} (n_S)^{2/3}, \quad (10)$$

where $\hbar$ is the reduced Planck's constant, ε_0 is the vacuum permittivity, and ε_{AlGaN} and m^* are the AlGaN dielectric constant and the AlGaN effective electron mass, respectively.

Then, by inserting the values of ΔE_C and ΔE_F in Eq. (8), it is possible to determine the experimental value of $\Phi_{B2}(0)$ for the heterostructure analyzed in this work, i.e., $\Phi_{B2}(0) = 0.28$ eV. It is worth noting that the same C-V analysis carried out by in the temperature range of 25–150 °C did not show any significant variation of the sheet carrier density n_S.

Fig. 5 shows the temperature dependence of the zero-bias Ni/AlGaN barrier height $\Phi_{B1}(0)$ determined using Eq.

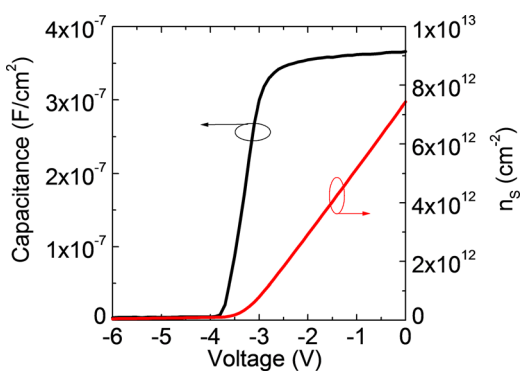

FIG. 4. Capacitance (left axis) and sheet carrier density n_S (right axis) of the 2DEG as a function of the applied voltage, determined by C-V measurements.

(6). As can be seen, the values of $\Phi_{B1}(0)$ determined with this approach increase with increasing the temperature, but they are lower than those extracted by the TE model (see Fig. 2), which had assumed the theoretical value of A^*. Moreover, the values of $\Phi_{B1}(0)$ in Fig. 5 are much lower than the theoretical one (which is independent of temperature) predicted by the Schottky–Mott relation $\Phi_B{}^{th} = \Phi_m - \chi_{AlGaN}$,[36] where Φ_m is the metal work function and χ_{AlGaN} is the AlGaN electron affinity, which in turns depends on the Al concentration.[2] In our case, considering an Al-concentration of our sample of 24%, an AlGaN affinity electron of 3.68 eV is obtained. Then, in the case of the Ni/AlGaN interface ($\Phi_m{}^{Ni} = 5.10$ eV), a theoretical barrier height $\Phi_B{}^{th} = 1.44$ eV is obtained. This value is reported for comparison as a dashed line in Fig. 5.

Now, as the zero-bias barrier height extrapolated with this method is affected by the strongly non-ideal behavior of the contact, to have a better description of our system we introduce the flat-band Schottky barrier height $\Phi_{FB} = \Phi_{B1}(V_{FB})$, i.e., the barrier height at zero electric field, which is a fundamental property depending only on the metal/semiconductor interface properties.

In order to determine the flat-band barrier height, it is useful to remind the correlation between the zero-bias and zero electric field barrier heights.[40] By adapting the approach proposed by Wagner *et al.*[40] to our AlGaN/GaN heterostructure, the flat-band barrier height Φ_{FB} can be written as a function of the two barriers as

$$\Phi_{FB} = n_1\Phi_{B1}(0) - (n_1 - 1)\Phi_{B2}(0). \quad (11)$$

Hence, inserting in Eq. (10) the temperature dependent values of the zero-bias Ni/AlGaN barrier $\Phi_{B1}(0)$ and the value of $\Phi_{B2}(0) = 0.28$ eV experimentally determined by C-V measurements enabled us to extract the values of $\Phi_{B1}(V_{FB})$ at each measurement temperature. These calculations led to values of Φ_{FB} almost independent of the temperature in all the investigated temperature range, i.e., $\Phi_{FB} \approx 1.40$ eV. It is worth noting that the experimental value of Φ_{FB} determined with this method is in closer agreement with the theoretical one predicted by the Schottky-Mott relation $\Phi_{B1}{}^{th} = 1.44$ eV for an Al concentration of 24% (dashed line in Fig. 5).

Finally, some further considerations can be done to corroborate the validity of this approach. Typically, metal/semiconductor barrier heights can be determined either by standard electrical measurements (I–V, C-V) or by more complex photoemission techniques.[41] The values of the barrier extracted by this latter technique are typically considered as the most reliable ones, as they do not depend on the effects of barrier inhomogeneity affecting the results of the electrical measurements.[41]

In Fig. 6, a survey of literature values of the Ni/AlGaN barrier height obtained by photoemission measurements[33,42,43] is reported, as a function of the Al-concentration. The experimental value found in this work by electrical measurements is also reported for comparison. In this graph, the dashed line represents the ideal barrier predicted by the Schottky-Mott relation. In particular, since the AlGaN electron affinity χ_{AlGaN} decreases linearly with increasing the Al concentration, i.e., $\chi_{AlGaN} = 4.20 - 2.15\ x_{Al}$ (eV),[2] the theoretical Schottky-Mott relation becomes $\Phi_{B1}{}^{th} = \Phi_m - \chi_{AlGaN} = \Phi_m - (4.20 - 2.15\ x_{Al})$ (eV). As can be seen, the results of this work are consistent with the literature photoemission measurements, confirming the usefulness of our method based on electrical analysis for a reliable determination of the barrier height in heterostructures.

IV. SUMMARY

The properties of the Ni/Au Schottky barrier on AlGaN/GaN heterostructures have been investigated at different temperatures. In particular, the forward I–V curves of Schottky diodes revealed a deviation from the ideal behavior, which cannot be explained by the thermionic emission model. Hence, the Ni/AlGaN/GaN system has been described by adapting a "two diode model," which takes into account the presence of a second barrier height for electrons at the AlGaN/GaN heterojunction. In this way, combining the I–V measurements with C-V measurements acquired to determine the experimental properties of the 2DEG made possible to extract the zero-bias barrier height of the Ni/

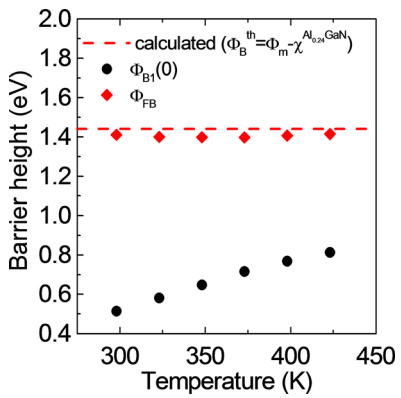

FIG. 5. Experimental temperature dependence of the zero-bias barrier height $\Phi_{B1}(0)$ and of the flat-band barrier height Φ_{BF} determined by the "two diode model." The dashed line represents the calculated barrier height according to the Schottky-Mott relation (which is independent of temperature) for an Al-concentration of 24%.

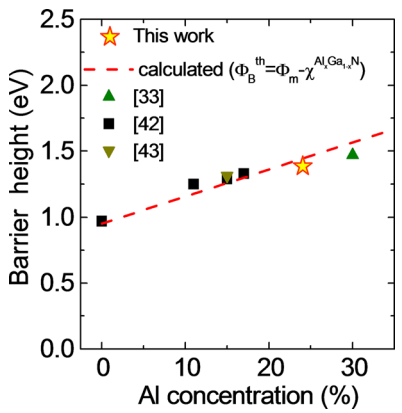

FIG. 6. Literature data of the Schottky barrier height for Ni/Au Schottky contacts to AlGaN/GaN heterostructures as a function of the Al-concentration, determined by photoemission measurements. Our experimental value, determined by electrical measurements, is also reported. The dashed line represents the theoretical dependence predicted by the Schottky-Mott relation.

AlGaN interface. The resultant value is, however, much lower than the theoretical one and strongly dependent on the temperature, thus indicating the presence of an inhomogeneous metal/semiconductor barrier. Hence, to have a more exhaustive description of the system, the flat-band Schottky barrier height Φ_{FB} has been introduced, which is an intrinsic property of the metal/semiconductor interface. The analyses of the temperature dependence forward I–V curves and C-V measurements with the "two diode model" resulted in an almost temperature independent flat-band barrier height of 1.40 eV. This value is consistent with the theoretical one predicted by the Schottky-Mott relation and is in good agreement with literature photoemission data.

The results provide a straightforward procedure for a reliable determination of the barrier height in AlGaN/GaN heterostructures by electrical measurements on Schottky diodes and can be very useful to understand and predict the final behavior of AlGaN/GaN HEMTs.

ACKNOWLEDGMENTS

The authors would like to acknowledge S. Di Franco (CNR-IMM) for his valuable assistance during device fabrication, and S. Reina and A. Parisi (STMicroelectronics) for help during electrical measurements. Moreover, the fruitful discussions with P. Fiorenza (CNR-IMM) and F. Iucolano (STMicroelectronics) were greatly appreciated during the elaboration of this paper. This work has been funded, in part, by the project "GraNitE: Graphene heterostructures with Nitrides for high frequency Electronics" (Grant No. 0001411) in the framework of the EU program "FET Flagship ERA-NET" (FLAG-ERA).

[1]M. Kuzuhara and H. Tokuda, IEEE Trans. Electron Devices **62**, 405 (2015).
[2]O. Ambacher, J. Smart, J. R. Shealy, N. G. Weimann, K. Chu, M. Murphy, W. J. Schaff, L. F. Eastman, R. Dimitrov, L. Wittmer, M. Stutzmann, W. Rieger, and J. Hilsenbeck, J. Appl. Phys. **85**, 3222 (1999).
[3]F. Roccaforte, P. Fiorenza, G. Greco, R. Lo Nigro, F. Giannazzo, A. Patti, and M. Saggio, Phys. Status Solidi A **211**, 2063 (2014).
[4]J. W. Chung, W. E. Hoke, E. M. Chumbes, and T. Palacios, IEEE Electron Devices Lett. **31**, 195 (2010).
[5]F. Ren and J. C. Zolper, *Wide Band Gap Electronic Devices* (World Scientific, Singapore, 2003).
[6]J. D. Guo, F. M. Pan, M. S. Feng, R. J. Guo, P. F. Chou, and C. Y. Chang, J. Appl. Phys. **80**, 1623 (1996).
[7]T. U. Kampen and W. Mönch, Appl. Surf. Sci. **117–118**, 388 (1997).
[8]P. Hacke, T. Detchprohm, K. Hiramatsu, and N. Sawaki, Appl. Phys. Lett. **63**, 2676 (1993).
[9]J. K. Kim, H. W. Jang, and J. L. Lee, J. Appl. Phys. **94**, 7201 (2003).
[10]C. Lu and S. Noor Mohammad, Appl. Phys. Lett. **89**, 162111 (2006).
[11]F. Roccaforte, F. Giannazzo, F. Iucolano, J. Eriksson, M. H. Weng, and V. Raineri, Appl. Surf. Sci. **256**, 5727–5735 (2010).
[12]L. S. Yu, Q. Z. Liu, Q. J. Xing, D. J. Qiao, S. S. Lau, and J. Redwing, J. Appl. Phys. **84**, 2099 (1998).
[13]J. Kotani, T. Hashizume, and H. Hasegawa, J. Vac. Sci. Technol. B **22**, 2179 (2004).
[14]A. R. Arehart, B. Moran, J. S. Speck, U. K. Mishra, S. P. DenBaars, and S. A. Ringela, J. Appl. Phys. **100**, 023709 (2006).
[15]Y. Zhou, D. Wang, C. Ahyi, C.-C. Tin, J. Williams, M. Parka, N. M. Williams, A. Hanser, and E. A. Preble, J. Appl. Phys. **101**, 024506 (2007).
[16]Y.-J. Lin, J. Appl. Phys. **106**, 013702 (2009).
[17]Y. Wang *et al.*, Semicond. Sci. Technol. **26**, 022002 (2011).
[18]M. L. Lee, J. K. Sheu, and S. W. Lin, Appl. Phys. Lett. **88**, 032103 (2006).
[19]F. Iucolano, F. Roccaforte, F. Giannazzo, and V. Raineri, J. Appl. Phys. **104**, 093706 (2008).
[20]N. Miura, T. Nanjo, M. Suita, T. Oishi, Y. Abe, T. Ozeki, H. Ishikawa, T. Egawa, and T. Jimbo, Solid-State Electron. **48**, 689 (2004).
[21]K. Shiojima, T. Suemitsu, and M. Ogura, Appl. Phys. Lett. **78**, 3636 (2001).
[22]J. Spradlin, S. Doğan, J. Xie, R. Molnar, A. A. Baski, and H. Morkoc, Appl. Phys. Lett. **84**, 4150 (2004).
[23]F. Iucolano, F. Roccaforte, F. Giannazzo, and V. Raineri, J. Appl. Phys. **102**, 113701 (2007).
[24]N. Miura, T. Oishi, T. Nanjo, M. Suita, Y. Abe, T. Ozeki, H. Ishikawa, and T. Egawa, IEEE Trans. Electron Devices **51**, 297 (2004).
[25]S. T. Bradley, S. H. Goss, J. Hwang, W. J. Schaff, and L. J. Brillson, J. Appl. Phys. **97**, 084502 (2005).
[26]S. Saadaoui, M. Mongi Ben Salem, M. Gassoumi, H. Maaref, and C. Gaquière, J. Appl. Phys. **110**, 013701 (2011).
[27]H. Zhang, E. J. Miller, and E. T. Yu, J. Appl. Phys. **99**, 023703 (2006).
[28]E. Arslan, S. Altindal, S. Özçelik, and E. Ozbay, J. Appl. Phys. **105**, 023705 (2009).
[29]D. Yan, J. Jiao, J. Ren, G. Yang, and X. Gu, J. Appl. Phys. **114**, 144511 (2013).
[30]A. F. M. Anwar and E. W. Faraclas, Solid-State Electron. **50**, 1041 (2006).
[31]T.-C. Nam, J.-S. Jang, and T.-Y. Seong, Curr. Appl. Phys. **12**, 1081 (2012).
[32]C. H. Chen, S. M. Baier, D. K. Arch, and M. S. Shur, IEEE Trans. Electron Devices **35**, 570 (1988).
[33]Y. Lv, Z. Lin, T. D. Corrigan, J. Zhao, Z. Cao, L. Meng, C. Luan, Z. Wang, and H. Chen, J. Appl. Phys. **109**, 074512 (2011).
[34]G. Greco, F. Iucolano, and F. Roccaforte, Appl. Surf. Sci. **383**, 324–345 (2016).
[35]F. Iucolano, F. Roccaforte, F. Giannazzo, and V. Raineri, Appl. Phys. Lett. **90**, 092119 (2007).
[36]E. H. Rhoderick and R. H. Williams, *Metal-Semiconductor Contacts* (Oxford Science, Oxford, 1988).
[37]F. Roccaforte, F. La Via, V. Raineri, R. Pierobon, and E. Zanoni, J. Appl. Phys. **93**, 9137 (2003).
[38]P. M. Gammon, A. Pérez-Tomás, V. A. Shah, O. Vavasour, E. Donchev, J. S. Pang, M. Myronov, C. A. Fisher, M. R. Jennings, D. R. Leadley, and P. A. Mawby, J. Appl. Phys. **114**, 223704 (2013).
[39]G. Martin, A. Botchkarev, A. Rockett, and H. Morkoç, Appl. Phys. Lett. **68**, 2541 (1996).
[40]L. F. Wagner, R. W. Young, and A. Sugerman, IEEE Electron Device Lett. **4**(9), 320 (1983).
[41]D. K. Schroder, *Semiconductor Material and Device Characterization* (John Wiley and Sons, New York, 1998).
[42]D. Qiao, L. S. Yu, S. S. Lau, J. M. Redwing, J. Y. Lin, and H. X. Jiang, J. Appl. Phys. **87**, 801 (2000).
[43]L. S. Yu, Q. J. Xing, D. Qiao, S. S. Lau, K. S. Boutros, and J. M. Redwing, Appl. Phys. Lett. **73**, 3917 (1998).